ISSN 1547-4771, Physics of Particles and Nuclei Letters, 2019, Vol. 16, No. 6, pp. 899–906. © Pleiades Publishing, Ltd., 2019.

PHYSICS AND TECHNIQUE OF ACCELERATORS

Innovative 20-MeV Superconducting Cyclotron for Medical Applications

V. Smirnov[a], *, S. Vorozhtsov[a], X. Wu[b], and J. Vincent[b]

[a]*Joint Institute for Nuclear Research, Dubna, Russia*

[b]*Ionetix corporation, Lansing, MI 48911, USA*

**e-mail: vsmirnov@jinr.ru*

Received July 28, 2019; revised August 9, 2019; accepted August 9, 2019

Abstract—The report contains a description of the conceptual design of a compact superconducting cyclotron, which can produce 20-MeV proton beam for isotopes production. The goal of the present project is to develop a machine that can be cost-effective, of small size and reliable in comparison with other particle accelerator systems aimed for producing proton beam of similar energy. Superconductivity is now a well established technology. Its application permits high magnetic field of the ultra-compact cyclotron that after careful system modeling and optimization can produce sufficiently good final beam parameters. The main parameters of the cyclotron, its design, and major stages of the development work are described in the report.

Keywords: cyclotron, superconductivity, computer simulation, beam dynamics, electromagnetic fields

DOI: 10.1134/S1547477119060529

1. INTRODUCION

There are a lot of medical tasks, which require using of proton beam with relatively high intensity (several hundreds of microamperes) and energy of 14–20 MeV for isotope production used both for diagnostics and direct treatment of cancer. For example, the hot topics of recent annual meetings of Society of Nuclear Medicine and Molecular Imaging (SNMMI) is using the isotopes like Actinium and Astatine, which emit alpha-particle in short range to kill cancer cells instead using proton and carbon machine directly. The latter have significant cost and required time to build. So, the need for alpha-particle emitter like ^{225}Ac and ^{211}At is building up in the community. One needs 14–20 MeV protons to produce Actinium and 25–29 MeV alpha-particles to produce Astatine. Since industrial machines will be dedicated to a single isotope – one machine to do both is not necessary. There are big market for these isotopes, and we are looking into design a new 20 MeV proton superconducting cyclotron with high intensity to make ^{225}Ac [1]. Our proposed Ion-20SC machine will have some capabilities to meet these needs once completed.

Thus, the installations having the compact sizes and small energy consumption are considered as the most demanded. A compact superconducting cyclotron, which can produce protons with energy from designated energy range, is under design at collaboration between Ionetix Corporation (Lansing, USA) and JINR (Dubna, Russia). The new project is a continuation of ION-12SC cyclotron [2] that was successfully developed and get in operation by this collaboration. Initially the new cyclotron was aimed to get protons with final energy of 14 MeV [3], but later it was decided to increase final energy to 20 MeV for covering larger diapason of isotopes, which can be produced. Main feature of the cyclotron is using of both external and internal injection. Switching of working regimes should be made with replacement of the cyclotron central region. Figure 1 gives an impression of the cyclotron under design.

The approach was decided on to initially perform commissioning of the machine with the internal ion source, and, then, the external ion source will be used for high intensity of the final beam. This permits usage of rather simple internal cold cathode PIG ion source for H^- production initially with more sophisticated central region structure required for external injection afterwards. This latter structure is on the margin of the technological ability for manufacturing presently.

An accelerated H^- ion after losing electron at a stripping foil is extracted as a proton from the cyclotron vacuum chamber. The beam extraction efficiency is close to 100% there. The method of the beam extraction allows variation of the beam final energy by changing of radial position of the extraction foil. The main project requirement implies more than 200 μA intensity of the final beam in the external injection regime. High magnetic field of the accelerator leads to a total weight of the machine being of less than 6 t, see Table 1 below. CIAE-type Cusp ion source [4] is con-

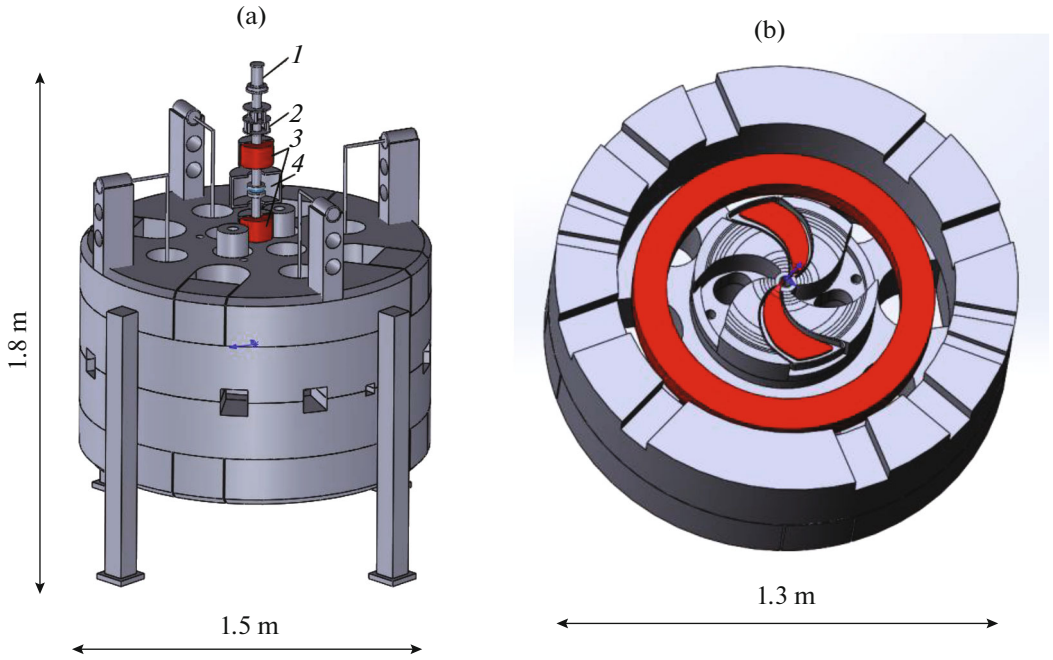

Fig. 1. Layout of the ION-20SC cyclotron. (a) Elements of axial injection line are shown: (*1*) ion source, (*2*) steerer, (*3*) solenoids, (*4*) buncher. (b) The median plane view: magnet yoke, coil, dees sectors are shown.

sidered for external injection of H^- beam having 9 mA (maximal) intensity at its exit. Concerning the internal ion source, the development described in [5] can be taken as an example to look at with the extracted beam current of 170 μA to rely on.

Table 1. Main cyclotron parameters

Cyclotron type	Compact, isochronous
Type of accelerated ion	H^-
Final beam energy	17–20 MeV
Output intensity of the beam	>200 μA
Injection type	External (Cusp), Internal (PIG)
Magnetic structure	4 spiral sectors
Central magnetic field	2.9 T
Hill gap	47–36–30 mm
Valley gap	230–140 mm
Accelerating system	2 spiral dees
Accelerating frequency	88 MHz
Accelerating mode	2
Peak dee voltage	30 kV
Extraction type	Stripping foil
Beam extraction radius	220 mm
Cyclotron diameter	1500 mm
Cyclotron height (with injection line)	1800 mm
Total weight	~6 t

2. MAGNETIC SYSTEM

Magnetic field level of the machine was chosen under several criteria, basic of which were: minimization of the accelerator size, providing of injection with acceptable beam transmission efficiency and focusing, possibility of practical realization of the cyclotron central region, and low particle losses by magnetic stripping. It can be seen in Fig. 2 that for central field level about 3 T and energy gain per turn provided by the selected RF system parameters the particle losses due to magnetic stripping are negligibly small up to the final ion energy of 20 MeV. As result field level of 2.9 T was selected eventually.

Magnetic system has four spiral sectors with maximal spirality of 50 degree (Fig. 1b). Isochronization of the average magnetic field is performed by variation of azimuthal size of the sectors, shaping of the axial gap between the sectors, and using the valley shims near the final radius. The magnetic structure designed ensures deviation of the calculated average magnetic field from the required isochronous dependence on radius less than ±15 G. The resulting value of axial betatron frequency reaches ~0.2 near the final radius. As an important constraint in the magnetic system design a minimal axial gap between the sectors of 30 mm was applied. Also, 500 mm cyclotron pole diameter was chosen for the structure. For the magnet configuration designed the engineering current density in the superconducting coil, immersed into a cryostat, should be ~85 A/mm^2 to provide the required magnetic field level. Given many cuttings in the magnet return yoke for moving in the spiral inflec-

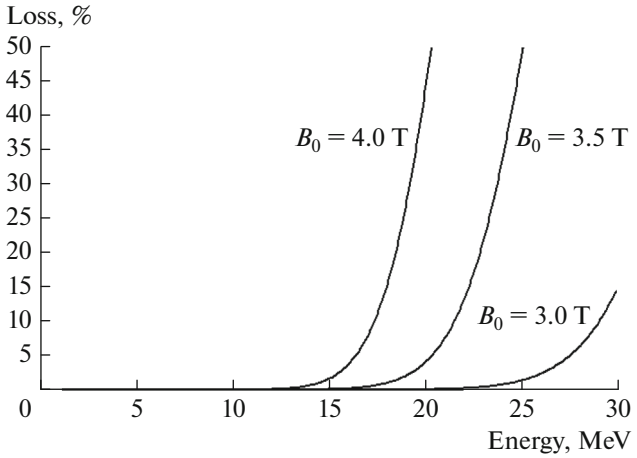

Fig. 2. Losses of H^- ions due to the magnetic stripping at energy gain 80 keV/turn depending on the final cyclotron energy and central magnetic field level.

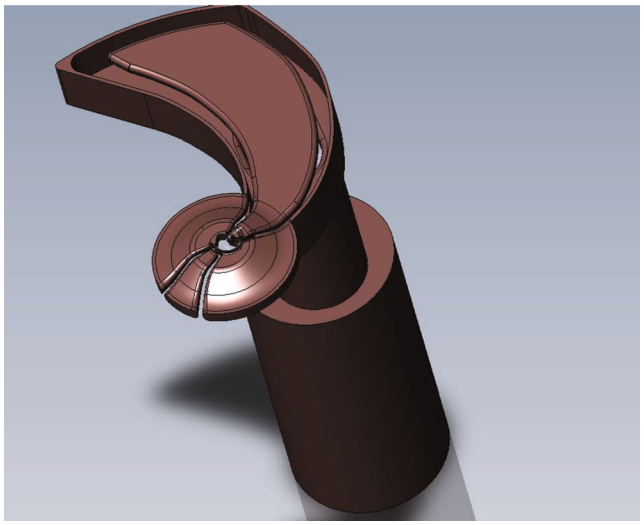

Fig. 3. The acceleration system structure with the central region, dee, and stem shown.

tor, the accelerating system, stripping foils, and the beam extraction elements, fringe magnetic field becomes lower than 500 G only at 600 mm distance from the yoke. So, only in this zone the stable operation of cryocoolers is possible. The vacuum chamber is intended to be stainless steel, or possible aluminum, bounded by caps filling the pole to sector axial gaps and walls of the cryostat. Vacuum required for suppressing losses due to H^- dissociation on gas can be in the 10^{-5} Torr range as in many existing accelerators using internal ion sources. The magnetic system utilizes a persistence switch at field. So, there are no conduction losses. However, the cryocooler must operate 24/7 and requires about 12 KW steady state power consumption.

3. ACCELERATING SYSTEM

Accelerating system consists of two spiral dees (Fig. 3) located in the valleys between the sectors. Peak dee voltage is limited by 30 kV providing a minimal power consumption of the facility. Axial aperture of the dees increases from 5 mm in the center to 30 mm in the rest of the radial range. This ensures an optimal accelerating field along the initial particles turns without sparking in axial direction between the surfaces of the magnetic system and the dees. The stems of the RF system are long enough to get through the magnet yoke. A lot of openings in the magnet core are required to accommodate the RF and other systems. Their size is large enough compared to the cyclotron dimensions lowering this way the magnetic field level as a result. The RF power is introduced to the acceleration system through some of the holes in the magnet caps—capacitive coupler and fine tuner and inductive course tuning stems. Calculations show about 5 KW is needed per dee at maximal voltage.

The beam central particle makes ~250 turns to reach final energy. In the external injection case the analysis of the beam centering shows on average the amplitude of radial betatron oscillations is near 2 mm. With slightly asymmetrical accelerating voltages on dees (30 kV—for the first dee, 28 kV—for the second dee) the amplitudes can be reduced to ~0.5 mm. For the internal ion source the average amplitude of radial betatron oscillations can be below ~1 mm.

4. AXIAL INJECTION LINE AND CORRESPONDING CENTRAL REGION

At the initial stage of the axial injection line development the existing information on the subject [6–8] was thoroughly investigated. In the design the main criteria were functionality, minimization of its dimensions, and relative simplicity of structure. On this way, preliminary calculations for a set of the transport lines were performed. As a result, a system consisting of two solenoids was selected. A similar structure is used in K500 superconducting cyclotron (Kolkata, India) [9], where a single long solenoid is located near the cyclotron yoke. The main idea of the approach is to take into account the longitudinal magnetic field of the cyclotron for required transverse focusing of the beam by choosing a corresponding axial opening in the magnet yoke. In this case the solenoids are used only for fine adjustment of the focusing process. Effective length of each solenoid was selected 90 mm and its aperture for the beam—40 mm. The calculated fields in the solenoids to match the beam to the central region acceptance are 0.7 and 1.0 kG with the field direction being opposite to the cyclotron's one. At the spiral inflector entrance used to bend the particles to the cyclotron midplane the transversal size of the

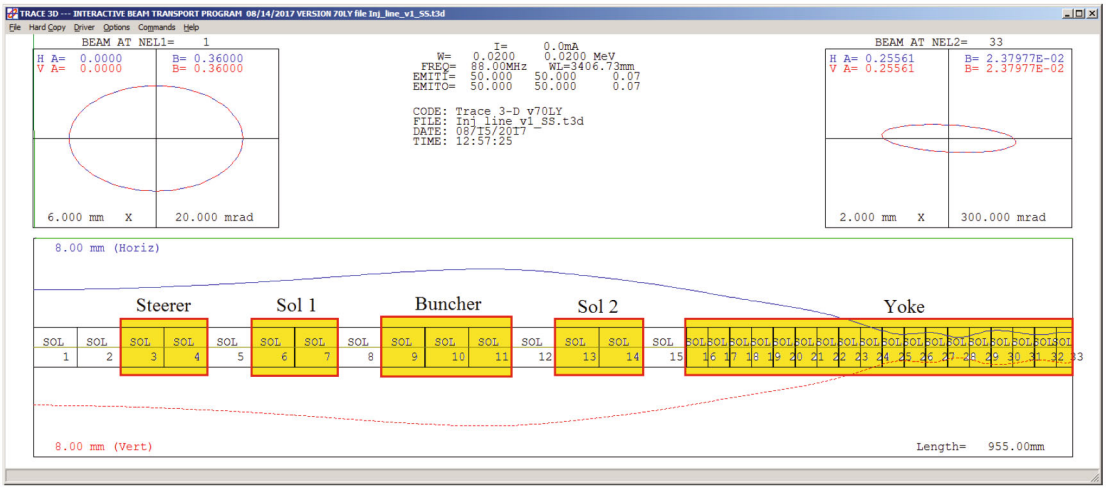

Fig. 4. Injection line beam transverse envelopes calculations.

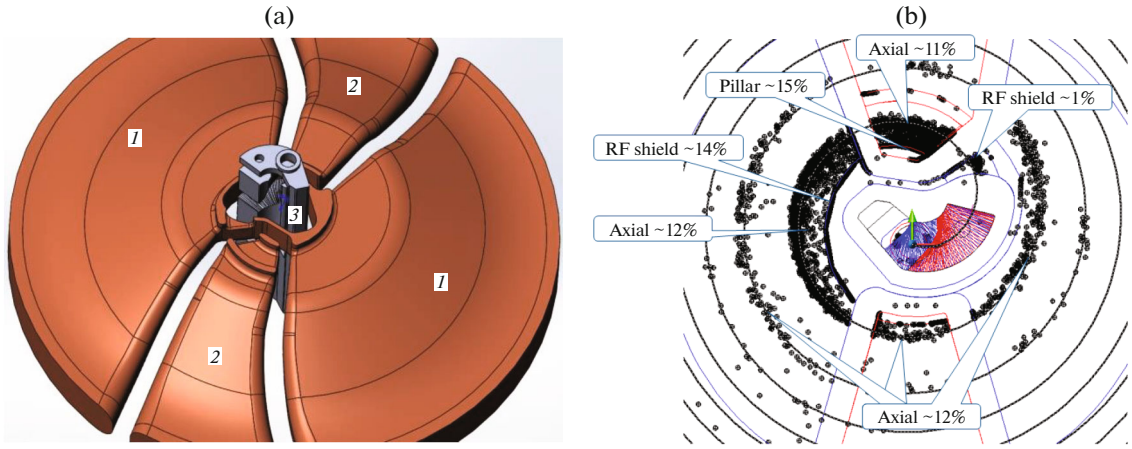

Fig. 5. (a) The central region structure in the external injection case. (b) Particle losses distribution in the structure: (*1*) dummy dee, (*2*) dee, (*3*) inflector unit configuration.

beam is below 2 mm. Parameters of the line were defined by calculations with matrix code Trace3D [10] (Fig. 4) following by checking the results by SNOP program complex [11]. In the line simulation it was assumed that the space charge forces were somehow compensated at ~80% level.

Measurements and calculations for existing compact cyclotrons show that installation in an axial injection line of a radio-frequency buncher with a *cos*-like dependence of voltage on time can increase the total beam transmission efficiency through a cyclotron up to three-four times [12]. Factor of the beam transmission increasing in case of using a buncher with sawtooth dependence of voltage is close to five. Given the electrical field of the buncher will be shaped by two sets of 50-μm-thick wires spaced by 3 mm, the grid transparency of ~98% and field nonuniformity in the working region of ~5% will be provided.

Detailed analysis of the *cos*-like buncher effect shows that the beam transmission through the cyclotron central region is increased from 12 to 34%. To decrease the beam radial losses, an optimal modification of the dee tips angular width was introduced. A sufficient axial focusing of the beam by RF field was provided by crossing the acceleration gaps at decreasing dee voltage, which was organized by an optimal positioning of the gaps.

The spiral inflector design permits its rotation around axial axis by several degrees to better matching of the injected beam to the accelerating region acceptance. The RF shielding box around the inflector mitigates the negative impact of the acceleration field to the beam passage though the unit (Fig. 5a). The calculations show that with the shielding box height being smaller than the inflector's one the beam transmission efficiency through the central region noticeably decreases due to deflection of particles by penetrating

accelerating field to the unit. The box is attached to the dummy dee and can be assembled with it as a single unit. There is sufficient room between the shield and inflector electrodes to put the potential connections and supporting elements for the inflector. Given the buncher is switch on in the injection line the particle losses (mostly radially) are ~66% in the central region (Fig. 5b). In this case the phase acceptance of the central region is about 40 degree RF.

A high magnetic field required for the cyclotron poses essential difficulties in designing the inflector having in mind necessity to minimize particle losses on the first turn. Increasing accelerating voltage can help in this sense but has a limited application due to existing constraint on its magnitude. So, the only practical method to sustain high enough beam transmission efficiency through the central region would be miniaturization of the inflector configuration. To this end, in the inflector design some normally applied recommendations to its parameters selection were revised. Optimization of the structure was conducted having in mind the beam dynamics aspects. Thus ratio of the inflector electrodes width to the value of gap between the electrodes was chosen to be 1.7 albeit normally it should be more than 2.0. Although this approach was proposed for some machines with the ratio being ~1.25 [13], but introduced this way electric field nonuniformity inside the inflector gap leads to substantial beam quality deterioration. Given maximal transmission efficiency of the beam through the central region takes place with the dee voltage being larger than the particle injection energy, the latter was chosen to be minimal for the ion source used, namely, 20 keV. The inflector gap is 3.5 mm, though usually it is about 4–6 mm in majority of operational cyclotrons. Electrical radius of the inflector is 10 mm with voltage on its electrodes being 14 kV and magnetic radius being 7 mm. With selected this way parameters the inflector assembly surrounding infrastructure included is extremely small (Fig. 6) causing substantial difficulties in its technical realization. The main problem is to provide sufficient space for placement the structure the potential connections including. The thickness of the electrodes isolating layers and ceramic isolators for electrodes attachments to the supports should be sufficiently large to withstand the voltage breakthrough to the ground. The total size of the inflector assembly including all infrastructure elements does not exceed 20 mm. Two schemes of potential connections to the inflector were considered. The first one provides connection of equal in absolute value, but opposite in sign potentials to electrodes of the inflector, shown in Fig. 6. The electrodes are fastened on a rod that is used for moving in and out of the inflector from the cyclotron center. This method requires ceramic insulators between the electrodes and the supports. The second possible scheme assumes

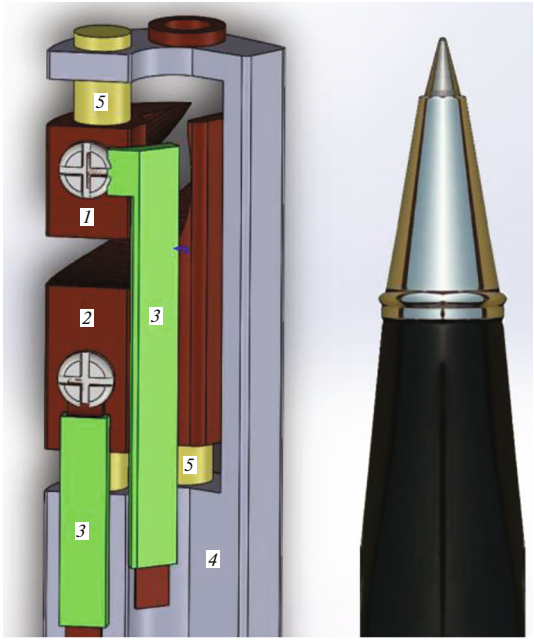

Fig. 6. 3-dimensional model of the spiral inflector in comparison to a standard pen: (*1*) upper electrode, (*2*) lower electrode, (*3*) potential connections, (*4*) electrode fixation, (*5*) ceramic isolators.

connection of potential to only one of the electrodes. The other electrode is at ground being fixed on a supporting structure.

An analysis of the inflector fringe field influence on the beam motion was performed considering some cutting of the electrodes edges to suppress the beam displacement from the electrode central line. In this case the amplitude of axial oscillations of the reference particle during acceleration is less than 0.2 mm.

5. CENTRAL REGION WITH INTERNAL ION SOURCE

As mentioned above, the cyclotron under design also needs an internal H^- ion source in addition to the external high intensity H^- one considered for the final configuration. This will be very useful for the initial commissioning of the machine. In this case the central region structure should be the same except the dee tips and the ion source replacing the inflector (Fig. 7). The central plug and all openings in the magnet yoke should meet requirements of both operation regimes. The beam centering should be sufficiently good with the value of amplitudes of radial betatron oscillations being less than 1–2 mm for both regimes.

PIG ion source, foreseen for the internal injection regime, has its slit size of 0.5×1 mm^2 and outer chimney radius of 2.5 mm (Fig. 8). It is enough to have an opening in the cyclotron return yoke with radius of 11 mm to axially introduce the ion source into the central region of the

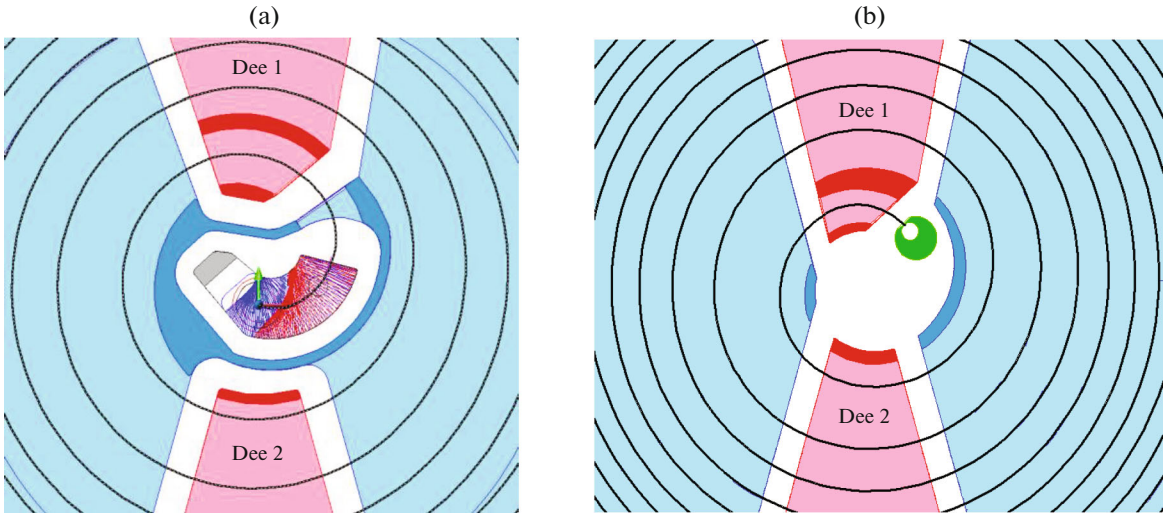

Fig. 7. Trajectory of the reference particle in the central region for the spiral inflector variant (a) and for the internal ion source regime (b).

machine. Based on existing test measurements for AMIT cyclotron ion source [5], the extracted beam intensity from a source for the machine under consideration can be taken about 50–60 μA when the source is installed in the cyclotron center.

The beam transmission through the central region is 30% with practically all particles losses being in horizontal plane. In this case the phase acceptance of the central region is 80 degree RF. Although in the external injection regime the phase slits do not practically increase the beam quality, for the internal ion source regime the situation looks different. In the latter case, one set of the phase slits improves the transverse beam quality along with suppressing the energy spread in the final beam by a factor of two but at expense of decreasing the beam transmission efficiency through the central region down to 22–25%.

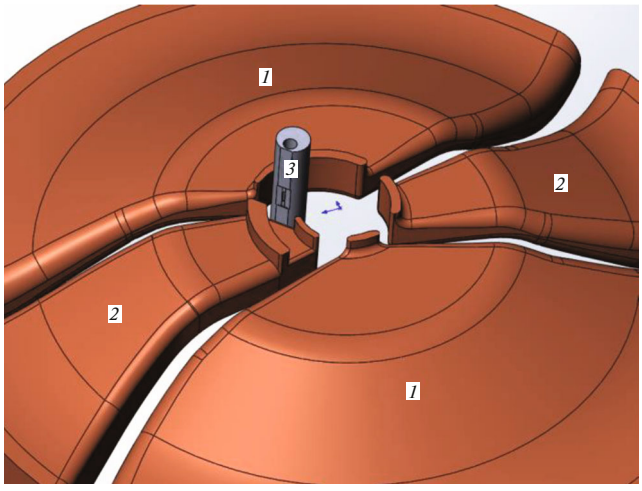

Fig. 8. Central region configuration for internal injection regime: (*1*) dummy-dee, (*2*) dee, (*3*) ion source.

6. EXTRACTON SYSTEM

It is planned to extract the beam from the cyclotron by stripping method through two extraction ports separated azimuthally by 180 degree. Stripping foils are available commercially nowadays and it seems there are no lifetime issues since they are widely used and presumably have been optimized. Displacement of the stripping foils radially permits some variation of the final beam energy in 17–20 MeV range. Further attenuation of the proton energy down to 14 MeV is possible by application of silver foils of varying thickness in the beam line outside the cyclotron. The azimuthal position of the foil is selected to trace the extracted beam through the region vacant of the dees. At each energy of the extracted beam a slight (about 1 deg) variation of the azimuthal position of the stripping foil ensures convergence of the particle trajectories to the same focus point outside the cyclotron (Fig. 9).

External targets for isotope production can be installed in a close vicinity to the cyclotron magnet yoke. The extracted beam from the cyclotron outlet windows to the targets can be transported, for example, by commercially available “Short port” lines [14] with their lengths of only 150 mm. The line configuration was developed and successfully applied for a number of GE PETtrace Series cyclotrons. It was found that the optimal transversal size of the final beam was ~10 mm for isotope production.

Beam dynamics analysis shows that to get the desired final beam intensity above 200 μA it is sufficient to ensure the extracted beam intensity from the external ion source of ~1 mA, although it can provide even higher

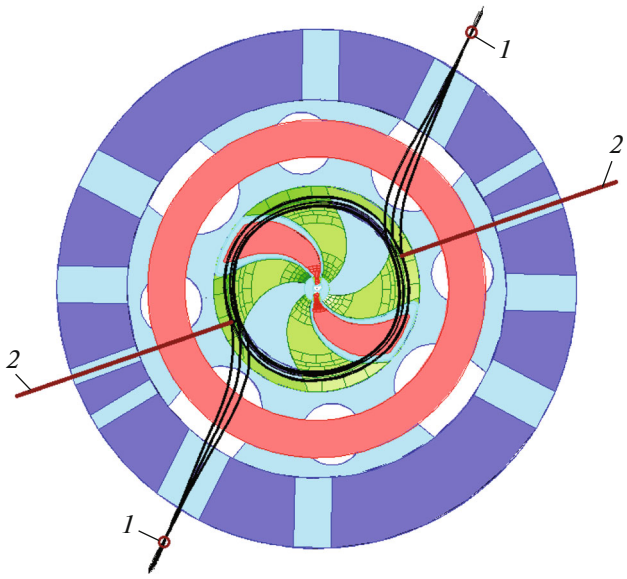

Fig. 9. Extracted particle trajectory: (*1*) convergence point for beams with extraction energy in 17–20 MeV range, (*2*) the rod for the striping foil position adjustment.

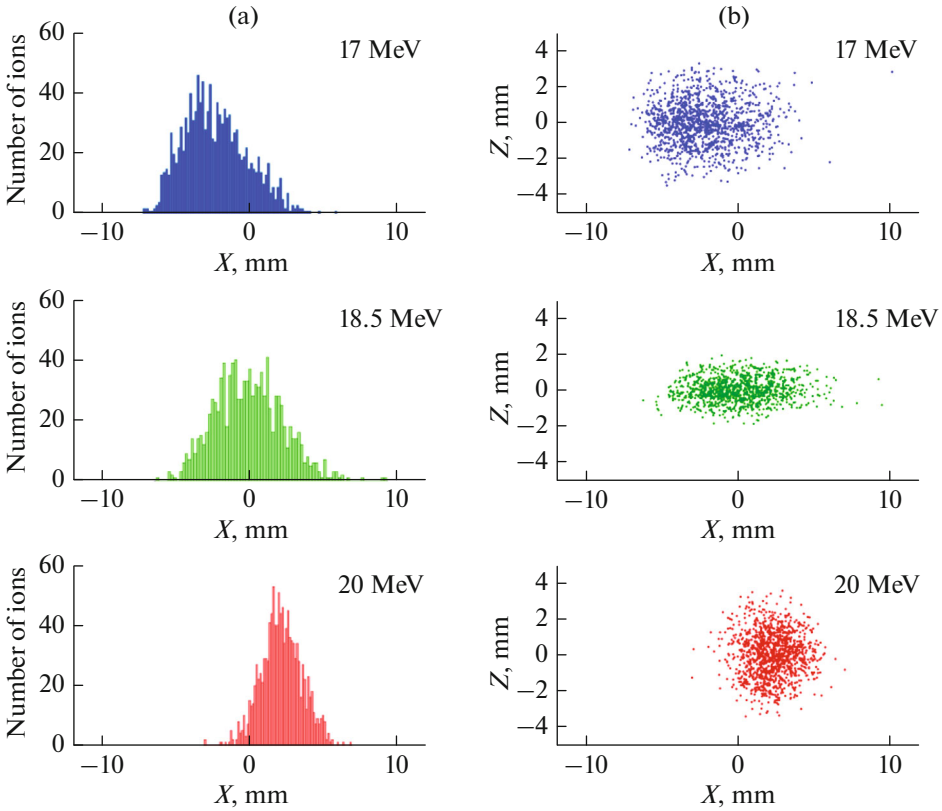

Fig. 10. External injection regime: (a) transverse distribution of protons and (b) beam spot at the focus point downstream the cyclotron for different energies of the final beam.

output beam of ~9 mA. In the internal source regime the final beam intensity of the cyclotron can reach ~15 μA. The transversal beam spots on the target are practically of the same size for both regimes, i.e., ~10 × 5 mm^2 (Fig. 10). There the horizontal and axial emittances are ~8 and ~3 π mm mrad respectively.

Table 2. Comparison of the ION-20SC cyclotron to in some machines for similar applications

	ION-20SC	Sumitomo HM-20	ACSI TR19	IBA Cyclone KIUBE	NIIEFA CC18
Accelerated ion	H^-	H^- (D^-)	H^- (D^-)	H^-	H^- (D^-)
Final beam energy, MeV	17–20	20 (10)	14-19 (9)	18	18 (9)
Final beam current, μA	>200	150 (40)	300 (100)	180	100 (50)
Number of extraction ports	2	2	2	8	2
Injection type	Cusp&PIG	PIG	Cusp	PIG	Cusp
Dimensions: diameter/height, m	1.3/0.7	2.6/1.7/2.0		1.9/1.8	1.7/1.8
Total weight, t	6	25	22	18	20
Power consumption, kW	~30	55	65	65	60
Central magnetic field, T	2.9	1.46	1.3	1.3	1.3
Peak dee voltage, kV	30	30	50	40	35
Cyclotron orientation	Horizontal	Vertical	Vertical	Horizontal	Vertical
Country	USA/Russia	Japan	Canada	Belgium	Russia

7. SUMMARY

The cyclotron developed has unique feature operating at high magnetic field for both external and internal injection regimes. Simulations performed at the design stage are most possible realistic and detailed ones taking into account the spatial distribution of the facility fields in calculating the accelerated particle trajectories. Careful optimization of all cyclotron systems permits obtaining sufficiently good efficiency of the beam transmission in the end-to-end (ion source to final focus) simulations of the beam acceleration for the parameters selected. The design of the magnetic and acceleration systems has a number of novel solutions that resulted in development of a cyclotron with weight and footprint by substantially (several times) smaller than for proposed and operational machines in similar energy range, see Table 2. Obviously, we are still at the conceptual design stage, and the detailed engineering of the machine is a subject of the future activity.

REFERENCES

1. M. Fukuda, "Novel cyclotron system for medical applications," in Proceedings of the AFAD2019 Conference.
2. J. Vincent, G. Blosser, G. Horner, K. Stevens, N. Usher, X. Wu, S. Vorozhtsov, and V. Smirnov, "The Ionetix ION-12SC compact superconducting cyclotron for production of medical isotopes," in Proceedings of Cyclotrons'16, Zurich, Switzerland, 2016.
3. V. L. Smirnov, S. B. Vorozhtsov, and J. Vincent, "H^- superconducting cyclotron for PET isotope production," Phys. Part. Nucl. Lett. **11**, 774–787 (2014).
4. Z. TianJue, J. XianLu, L. ZhenGuo, L. Yinlong, Q. JiuChang, Z. Xia, Y. Hongjuan, Z. JunQing, P. GaoFeng, G. Tao, and G. Fengping, "Development of series H^- multicusp ion source at China Institute of Atomic Energy," Rev. Sci. Instrum. **85**, 02B110 (2014).
5. D. Obradors et al., "Characterization of the AMIT internal ion source with a devoted dc extraction test bench," in Proceedings of IPAC2017, Copenhagen, Denmark, pp. 1740–1742.
6. T. Kuo, R. Baartman, et al., "A comparison of two injection line matching sections for compact cyclotrons," IEEE **3**, 1858, (1995).
7. Dong Hyun An et al., "Beam simulation of SQQ injection system in KIRAMS-30 cyclotron," in Proceedings of the EPAC 2006, Edinburgh, Scotland.
8. M. Dehnel and T. Stewart, "An industrial cyclotron ion source and injection system," in *Proceedings of CYCLOTRONS 2004, Tokyo, Japan, 2004,* pp. 293–295.
9. M. K. Dey et al., "Beam injection system of the KOLKATA superconducting cyclotron," in *Proceedings of CYCLORONS 2007, Giardini Naxos, Italy, 2007,* pp. 346–348.
10. K. Crandall and D. Rusthoi, "TRACE 3-D Documentation," 3rd ed., Report LA-UR-97-886 (Los Alamos National Laboratory, 1997), p. 106.
11. V. L. Smirnov and S. B. Vorozhtsov, "SNOP - beam dynamics analysis code for compact cyclotrons," in *Proceedings of the XXIII Russian Accelerator Conference, RuPAC'2012, St. Petersburg, Russia, 2012,* pp. 325–327.
12. J. Stetson, G. Machicoane, D. Poe, and F. Marti, "Intense beam operation of the NSCL/MSU cyclotrons," in *Proceedings of CYCLOTRONS 2010, Lanzhou, China, 2010,* pp. 27–32.
13. A. Garonna, "Cyclotron designs for ion beam therapy with cyclinacs," PhD Thesis (Ecole Polytech. Fed., Lausanne, 2011).
14. J. E. Theroux et al., "A 'short port' beam line for mounting custom targets to a GE PetTrace cyclotron," in *Proceedings of CYCLOTRONS 2007, Giardini Naxos, Italy, 2007.*